Superconductivity and spin fluctuations in {Th,U}Pt_4Ge_{12} skutterudites

E. Bauer,[1] Xing-Qiu Chen,[2,5] P. Rogl,[2] G. Hilscher,[1] H. Michor,[1] E. Royanian,[1] R. Podloucky,[2] G. Giester,[3] O. Sologub,[4] and A. P. Gonçalves[4]

[1]*Institute of Solid State Physics, Vienna University of Technology, A-1040 Wien, Austria*

[2]*Institute of Physical Chemistry, University of Vienna, A-1090 Wien, Austria*

[3]*Institute of Mineralogy and Crystallography, University of Vienna, Althanstrasse 14, A-1090 Wien, Austria*

[4]*Departamento de Química, ITN/CFMCUL, E.N. 10, P-2686-953 Sacavém, Portugal*

[5]*School of Materials and Metallurgy, Northeastern University, Shenyang, 110004, People's Republic of China*

(Received 14 April 2008; revised manuscript received 10 June 2008; published 21 August 2008)

Merging experimental data and *ab initio* calculations, we report on $ThPt_4Ge_{12}$ and UPt_4Ge_{12} as further members of germanium-based skutterudites. For $ThPt_4Ge_{12}$ electron-phonon coupled superconductivity develops below T_c=4.75 K, ascribed to intrinsic features of the Pt-Ge framework where Ge-*p* states dominate the electronic structure at the Fermi energy. Ruderman-Kittel-Kasuya-Yosida coupling via the Ge framework is too weak to enable magnetic ordering in nonsuperconducting UPt_4Ge_{12}.

DOI: 10.1103/PhysRevB.78.064516 PACS number(s): 74.70.Dd, 82.75.−z, 65.40.−b

I. INTRODUCTION

Recently we have described the formation, crystal structure, and superconducting properties of a class of skutterudite compounds {Sr,Ba,Eu}Pt_4Ge_{12} with a unique [Pt_4Ge_{12}] framework.[1–3] It was shown that below about T_c=5 K, electron-phonon coupled superconductivity (SC) emerges for the alkaline-earth compounds, ascribed to intrinsic features of the Pt-Ge framework where Ge-*p* states dominate the electronic structure at the Fermi energy. From density-functional theory (DFT) calculations it was inferred that although strongly localized Eu-4*f* states with their peak at 2 eV below the Fermi energy give rise to a local magnetic moment of 7μ_B in $EuPt_4Ge_{12}$, the Eu-*f* states do not hybridize and do not induce any spin polarization onto their neighbors and thus long-range magnetic order can only arise at very low temperatures below 1.7 K. As a unique class of Ge-based skutterudites was found to extend to 4*f*-electron systems {La,Ce,Pr,Nd}Pt_4Ge_{12},[4] the aim of the present work is a study of the phase formation and crystal structure as well as the characterization of bulk properties by means of resistivity, magnetization, specific-heat, and band-structure calculations for actinoid compounds {Th,U}Pt_4Ge_{12}.

While, in general, Th-based systems are in a nonmagnetic 4^+ state, (electronic configuration $5f^0 6s^2 p^2$), thus behaving like simple systems, the ground state of U is dominated by the partial occupation of the 5*f* shell giving rise to a rich variety of magnetic features such as long-range magnetic order or scenarios where the Stoner criterion is just not fulfilled.[5] The latter may provoke magnetic spin fluctuations, which may be revealed from the characteristic $T^3 \ln T$ contribution to the heat capacity at low temperatures.

One of the key questions in the formation of Ge-based skutterudites concerns the fact whether the addition of electrons, e.g., from Th^{4+} to the [Pt_4Ge_{12}] sublattice will create stable compounds and modify the electronic density of states (DOS) to enhance SC or drive the system toward semiconducting behavior.

II. EXPERIMENTAL DETAILS

Alloys of {Th,U}Pt_4Ge_{12} were prepared by argon arc melting. While $ThPt_4Ge_{12}$ specimen was subsequently heat treated in evacuated quartz capsules at 800 °C for two weeks, UPt_4Ge_{12} has to be directly quenched from the melt with nominal composition $U_{0.8}Pt_4Ge_{12}$. Phase purity and lattice parameters were derived from x-ray diffraction indicating single-phase conditions for $ThPt_4Ge_{12}$ but a small amount of nonmagnetic secondary phases (Ge+$PtGe_2$) for UPt_4Ge_{12}.

Bulk properties of these skutterudites were obtained by a number of standard techniques, details are summarized below. A superconducting quantum interference device magnetometer served for the determination of the magnetization from 2 up to 300 K in fields up to 6 T, comparing field-cooled and zero-field-cooled results. Specific-heat measurements on samples of about 1 g were performed at temperatures ranging from 1.5 up to 170 K by means of a quasiadiabatic step heating technique in external fields up to 0.2 T. The electrical resistivity was measured on bar-shaped samples using a four-probe dc method in the temperature range from 1.9 K to room temperature.

DFT was applied using the Vienna *ab initio* simulation package (VASP) (Refs. 6 and 7) with a relativistic spin-orbit coupling approach.[8,9] The Brillouin zone was sampled with $5\times5\times5$ Monkhorst-Pack $\vec{k}$-point grids. The exchange-correlation functional was treated within the generalized gradient approximation utilizing the approach of Ref. 10.

III. RESULTS AND DISCUSSION

The crystal structure of $ThPt_4Ge_{12}$ (from Rietveld refinements) and UPt_4Ge_{12} (from Kappa-CCD single-crystal x-ray data at 300, 200, and 100 K) was found to be cubic and isotypic with the filled skutterudite-type $LaFe_4Sb_{12}$.[11] Structure and lattice parameters are collected in Table I. Occupation factors were refined, corresponding to a full occupancy of the actinoid Pt and Ge sublattices. Although the Ge icosahedra are significantly smaller than the corresponding Sb framework and therefore effective bonding between the framework cages and the Th-center atoms is ensured, temperature-dependent single-crystal x-ray data for UPt_4Ge_{12} unambiguously defined a strong temperature dependency of

TABLE I. Crystallographic properties at 300 K of $ThPt_4Ge_{12}$ and UPt_4Ge_{12}, which both crystallize in the skutterudite structure: space group Im $\bar{3}$ (No. 204); Th and U are at 2(*a*) (0,0,0) sites, Pt at 8(*c*) $(\frac{1}{4},\frac{1}{4},\frac{1}{4})$ sites, and Ge at 24*g* $(0,y,z)$ sites. U_{eq} is a mean value of the atomic displacement ellipsoid and ϵ is the residual electron density in [el/nm^3].

Property	$ThPt_4Ge_{12}$	UPt_4Ge_{12}
Lattice parameter *a* @ 300 K [nm]	0.85931(3)	0.85887(4)
Ge 24*g* site: *y*	0.1515(3)	0.15048(9)
Ge 24*g* site: *z*	0.3556(3)	0.35275(9)
$R_{F2}=\Sigma\lvert F_o^2-F_c^2\rvert/\Sigma F_o^2$	0.057	0.026
max and min $\epsilon[\times 10^3]$	—	3.1; −1.95
U_{eq}(Th,U) [nm^2]; $U_{11}=U_{22}=U_{33}$	0.00012(1)	0.000210(3)
U_{eq}(Pt) [nm^2]; $U_{11}=U_{22}=U_{33}$	0.00009(1)	0.000097(3)
U_{eq}(Ge) [a] [nm^2]	0.00010(2)	0.000102(2)

[a] $U_{11}=0.0079(4), U_{22}=0.01131(4), U_{33}=0.01134(3),$ $U_{23}=0.0004(2),\ U_{12}=U_{13}=0.0;$ in nm^2.

atomic displacement parameters (ADP) in the temperature region from 100 to 300 K for the smaller uranium atoms (see Fig. 1). Thus typical rattling modes caused by uranium as filler atoms are derived from the atom displacement parameters

$$U_{ii}=\frac{\hbar^2}{2m_U k_B \theta_{E,ii}}\coth\left(\frac{\theta_{E,ii}}{2T}\right) \quad (1)$$

obtained from structure refinement at three different temperatures yielding an Einstein temperature of $\theta_E \approx 59$ K (m_U is the mass of uranium). The optimized structural parameters obtained from DFT calculations are in reasonable agreement with x-ray structure data (differences of $<1\%$).

Temperature-dependent resistivity measurements carried out on $ThPt_4Ge_{12}$ indicate SC at $T_c \approx 4.8$ K [compare Figs. 2(a) and 2(b)] while results for UPt_4Ge_{12} do not exhibit SC down to 1.9 K [Fig. 2(a)]. This significant difference in the ground states of both neighboring compounds is already reflected in the temperature dependencies of the resistivity in the normal-state region. Neither of the compounds, however, show a simple metal-like resistivity behavior, i.e., the Bloch-Grüneisen formula is not applicable in any case. Such a behavior is known for many superconductors and may be attributed to a substantial electron-phonon interaction strength responsible for the formation of Cooper pairs in conventional superconductors. Rather, the overall $\rho(T)$ dependence of $ThPt_4Ge_{12}$ follows the phenomenological model of Woodard and Cody,[12] which initially applied to A15 superconductors such as Nb_3Sn. Least-squares fits to this model are shown as solid line in Fig. 2(a), revealing reasonable agreement with a characteristic temperature $T_0=131$ K. Similar characteristic temperatures as well as similar but slightly lower transition temperatures into the superconducting state were observed recently for isomorphous $\{Sr,Ba\}Pt_4Ge_{12}$.[1] The residual resistivity $\rho_0 \approx 3\ \mu\Omega$ cm indicates good sample quality as well as the complete filling of the voids by Th in the skutterudite structure.

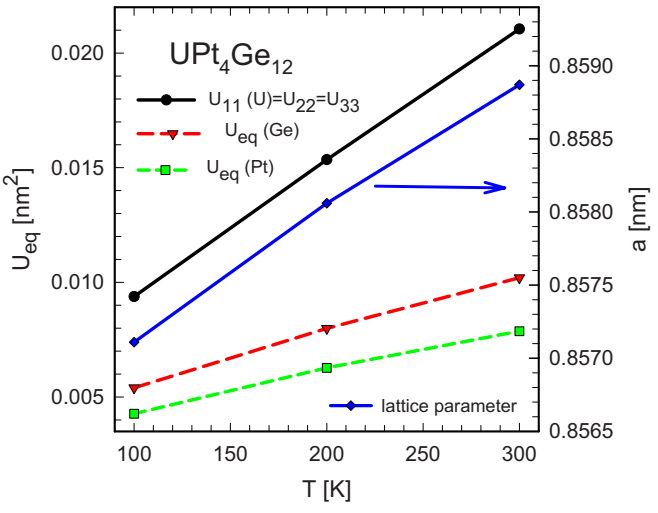

FIG. 1. (Color online) Temperature-dependent atom displacement parameters U_{eq} of the independent atom sites and lattice parameter σ of UPt_4Ge_{12}. The solid line is a guide to the eye.

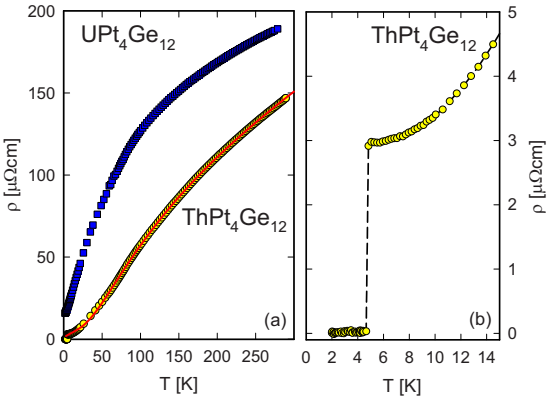

FIG. 2. (Color online) (a) Temperature-dependent electrical resistivity ρ of $ThPt_4Ge_{12}$ and UPt_4Ge_{12}. The solid line is a least-squares fit as explained in the text. (b) Low-temperature resistivity details evidencing superconductivity of $ThPt_4Ge_{12}$.

The overall $\rho(T)$ features of UPt_4Ge_{12} turn out to be different. At low temperatures, $\rho(T)$ behaves according to $\rho(T)=\rho_0+AT^n$ with $\rho_0=14.5\ \mu\Omega$ cm, $A=0.42\ \mu\Omega$ cm/K$^{1.5}$, and $n=1.5$. The latter refers to distinct deviations from a Fermi-liquid ground state due to strong spin fluctuations, which are evident also from a large value of the Sommerfeld constant $\gamma=156$ mJ/mol K^2 (see below). Moreover, classical spin fluctuation systems such as YCo_2 exhibit—at elevated temperatures—a tendency toward saturation, which can also be conceived from Fig. 2(a) for UPt_4Ge_{12}.

The magnetic susceptibility χ of $ThPt_4Ge_{12}$ (see Fig. 3) is diamagnetic in the normal-state region, revealing a temperature-independent susceptibility $\chi=-1.5\times10^{-7}$ cm^3/g. At $T=4.8$ K the sharp transition provides evidence for SC, in perfect agreement with the resistivity data. The diamagnetic value of $[-1/4\pi]$ for zero-field cooling corresponds to a complete flux exclusion of the total sample volume due to the screening currents. The flux expulsion (Meissner-Ochsenfeld effect) for field cooling in 50 and 200 G is only 21% and 17% of the shielding signal, which indi-

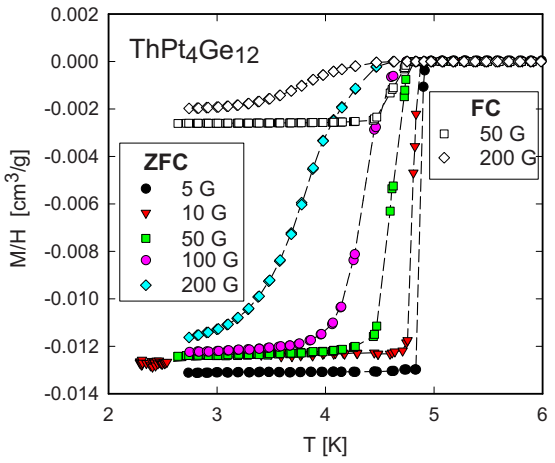

FIG. 3. (Color online) Temperature-dependent susceptibility M/H of $ThPt_4Ge_{12}$. The jump at $T=T_c$ for 5G reveals a full Meissner effect. Filled and open symbols refer to zero field and field cooling, respectively.

cates a rather strong flux pinning in a type II superconductor. With growing external fields the transition is washed out and shifted to lower temperatures and is suppressed in fields larger than 0.13 T above 2.2 K.

The heat capacity C_p of $ThPt_4Ge_{12}$ is plotted in Fig. 4 as C_p/T vs T for various fields up to 0.2 T. The jump of $C_p(T)$ below 5 K evidences bulk SC. Idealizing the specific-heat anomaly under the constraint of entropy balance between the superconducting and the normal state, we arrive at T_c =4.75 K. The entropy balance between the superconducting and the normal state defines $C_p/T(T=0)=35(1)$ mJ/mol K^2 and, furthermore, the heat capacity in the superconducting [dashed-dotted line in Fig. 4(a)] and in the normal state [dashed line in Fig. 4(a)] (i.e., measurements at 0 and 0.2 T, respectively), indeed yields $\Delta S(T=T_c)=0$. To derive these extrapolations, the phonon contribution is taken from the model sketched in Fig. 5 (see discussion below). The BCS

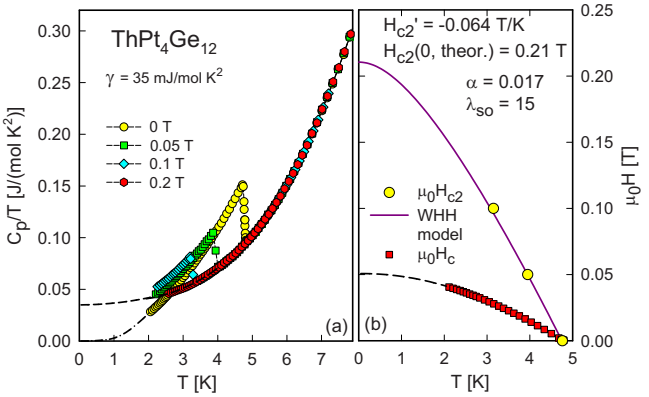

FIG. 4. (Color online) (a) Temperature-dependent specific heat C_p of $ThPt_4Ge_{12}$ plotted as C_p/T vs T for various externally applied magnetic fields. The dashed and the dashed-dotted lines are extrapolations from the normal and superconducting states, respectively. (b) Upper critical field $\mu_0 H_{c2}$ of $ThPt_4Ge_{12}$. Data are taken from the heat-capacity data. The solid line corresponds to the WHH model as explained in the text.

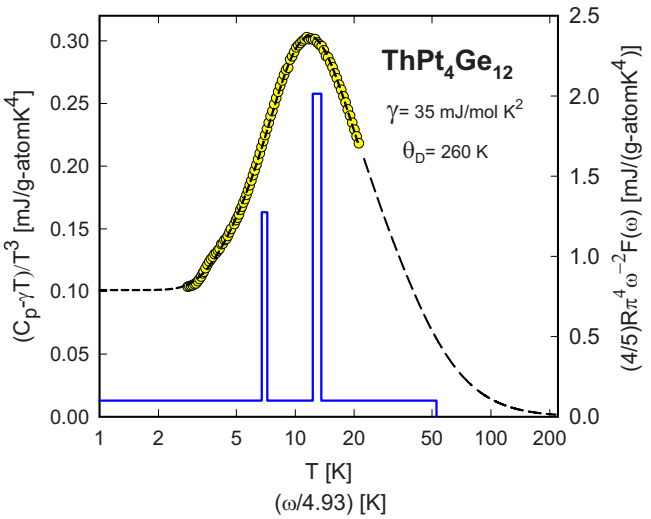

FIG. 5. (Color online) Temperature-dependent specific heat C_p of $ThPt_4Ge_{12}$ plotted as $(C_p-\gamma T)/T^3$ vs ln T. The dashed line is a least-squares fit of the experimental data using the model described in the text with a Debye spectrum (θ_D=260 K) and two Einstein-type modes (ω_{EL1}=34.7 K with a width of 2.2 K and ω_{EL2} =63.8 K with a width of 6.4 K). The solid line (referring to the right axis) describes the phonon spectral function $F(\omega)$ plotted as $(4/5)R\pi^4\omega^{-2}F(\omega)$ vs $\omega/4.93$. ω is given in degrees kelvin.

equation $C_{eS}(T)=8.5\gamma T_c \exp(-0.82\Delta(0)/k_B T)$ is applied in order to describe the electronic contribution to $C_p(T)$ in the superconducting state [dashed-dotted line, Fig. 4(a)]. Here, $\Delta(0)$ represents the superconducting gap at $T=0$.

The inapplicability of a Debye-type extrapolation of $C_p(T)$ toward low temperatures (as usually applied in simple metallic systems) demonstrates the existence of a complicated phonon spectrum in this compound.

For a qualitative and quantitative description of the lattice dynamics, we adapted a model comprising some fine structure in the phonon DOS $F(\omega)$.[13,14] Accordingly, the heat capacity is

$$C_{ph}(T) = 3R\int_0^\infty F(\omega)\frac{\left(\frac{\omega}{2T}\right)^2}{\sinh^2\left(\frac{\omega}{2T}\right)}d\omega, \qquad (2)$$

with ω the phonon frequency and R the gas constant. The most common assumptions on $F(\omega)$ are $F(\omega)=\delta(\omega)$ and $F(\omega)\sim\omega^2$ up to a cut-off frequency ω_D, corresponding to the well-known Einstein and Debye model, respectively. Junod *et al.*[13] demonstrated that certain functionals of the phonon specific heat take the form of convolutions of the phonon spectrum. In particular, $(5/4)R\pi^4 C_{ph}T^{-3}$ is an image of the spectrum $\omega^{-2}F(\omega)$ for $\omega=4.93T$, where ω is expressed in degrees kelvin. Based on these considerations we have constructed an elementary phonon spectrum and have carried out least-squares fits to the data. Besides a Debye DOS, we assumed that the system contains two additional energetically separated Einstein-type modes ω_1 and ω_2. In contrast to the standard Einstein model of the specific heat, a certain

frequency width $\Delta\omega$ for each of these branches is allowed. Results of this ansatz are shown in Fig. 5 as dashed line.

Based on this fit, the phonon spectra are constructed and plotted in Fig. 5 referring to the right axis (solid line). The spectral weight follows from the constraint that for $T\rightarrow 0$ the height of the phonon DOS coincides with the value of C_p/T^3 for $T\rightarrow 0$. The low-lying phonon branch may render those lattice vibrations which couple to the electron system, thereby enabling BCS-type SC.

Within the McMillan model,[15] the superconducting transition temperature T_c is given by

$$T_c = \frac{\theta_D}{1.45}\exp\left[\frac{-1.04(1+\lambda)}{\lambda-\mu_c^*(1+0.62\lambda)}\right], \quad (3)$$

where λ is the dimensionless electron-phonon coupling constant related in terms of the Eliashberg theory to the phonon DOS. λ determines the attractive part of the Cooper pair bonding while μ^* is the repulsive screened Coulomb part, usually set to ≈ 0.13. Applying this simple model yields $\lambda = 0.66$, referring to superconductors beyond the weak-coupling limit.

Taking the jump of the specific heat $\Delta C_p/T(T=T_c) = 61(2)$ mJ/mol K^2, $\Delta C_p/(\gamma_n T_c)$ is calculated to be ≈ 1.75, which is above the value expected from the BCS theory $[\Delta C_p/(\gamma T_c)\approx 1.43]$. As the magnetic-field strength increases, both the transition temperature and the anomaly right at T_c are suppressed, defining the phase diagram shown in Fig. 4(b).

The superconducting gap $\Delta(0)$ of $ThPt_4Ge_{12}$ can be estimated from the modified BCS expression $C_{eS}(T) = 8.5\gamma T_c \exp[-0.82\Delta(0)/k_B T]$. Adjusting this model expression to our specific-heat data at lowest temperatures, $C_{eS}(T)=C_p(T)-C_{ph}(T)$ reveals $\Delta = 0.72(1)$ meV. The ratio $\Delta(0)/k_B T_c \simeq 1.8$ is in fine agreement with the BCS value $\Delta_{BCS}(0)=1.76 k_B T_c$.

The thermodynamic critical field is calculated from the free-energy difference between the superconducting and normal state: $\Delta F(T)=F_n-F_s=\mu_0 H_c^2(T)/2=\int_{T_c}^{T}\int_{T_c}^{T'}\frac{(C_s-C_n)}{T''}dT''dT'$. $C_s(T)$ is obtained from the zero-field specific-heat measurement and $C_n(T)$ is taken from the 0.2-T data. The values obtained are displayed in Fig. 4(b) (filled squares); an extrapolation $T\rightarrow 0$ yields $\mu_0 H_c(0)\approx 50$ mT, very similar to the figures derived for $\{Sr,Ba\}Pt_4Ge_{12}$.[1]

Figure 4(b) displays the temperature-dependent upper critical field $\mu_0 H_{c2}$ of $ThPt_4Ge_{12}$ as deduced from $C_p(T,H)$. Data derived from magnetization measurements are found to correspond within the error bars. The slope of the upper critical field is $\partial(\mu_0 H_{c2})/\partial T \equiv \mu_0 H_{c2} = -0.064$ T/K.

Essentially two mechanisms limit the value of $\mu_0 H_{c2}$: orbital pair breaking and Pauli limiting. Werthamer *et al.*[16] derived an expression (Werthammer, Helfand, Hohenberg, WHH, model) for the upper critical field $\mu_0 H_{c2}$ in terms of orbital pair breaking, including the effect of Pauli-spin paramagnetism and spin-orbit scattering. A comparison of the experimental results with the WHH model is based on two parameters: α, the Pauli paramagnetic limitation (*Maki parameter*) and λ_{so} describing spin-orbit scattering. If the atomic numbers of the elements constituting the material increase, λ_{so} is expected to increase as well.

The Maki parameter α can be estimated from the Sommerfeld value γ and ρ_0 (Ref. 16) $\alpha=(3e^2\hbar\gamma\rho_0)/(2m\pi^2 k_B^2)$ with e the electron charge and m the electron mass. Taking the experimental ρ_0 and γ yields $\alpha=0.017$ for $ThPt_4Ge_{12}$. A value of similar magnitude can be derived from $\alpha = 5.3\times 10^{-5}[\frac{-dH_{c2}(T)}{dT}]|_{T=T_c}$.[17]

An increasing value of α reduces H_{c2} from the upper limit $h^*=H_{c2}/(T_c\partial\mu_0 H_{c2}/\partial T|_{T=T_c})=0.693$. Spin-orbital scattering, on the contrary, compensates for the decrease due to the paramagnetic limitation and restores $h^*\approx 0.693$ for $\lambda_{so}\rightarrow\infty$. Wong *et al.*[18] pointed out that $\lambda_{so}>10$ for $5d$ compounds, which also should hold for the present Pt-based system. We have adjusted the WHH model to the experimental data [solid line in Fig. 4(b)], revealing $\lambda_{so}\approx 15$. Note, however, $H_{c2}(T\rightarrow 0)$ is quite insensitive for $\lambda_{so}>10$. Both enhancement effects as well as strong coupling are expected to have only minor influence on these data.[18]

The thermodynamic and the upper critical fields are used to calculate the ratio of the penetration depth $\lambda_{GL}(0)$ to the coherence length $\xi_{GL}(0)$ via Abrikosov's relation $\lambda_{GL}(0)/\xi_{GL}(0)\equiv\kappa_{GL}(0)=H_{c2}/[\sqrt{2}H_c(0)]$ yielding the Ginzburg-Landau parameter $\kappa_{GL}\approx 3$. The absolute values of the coherence length ξ_0 and the penetration depth $\lambda(0)$ can be evaluated via the isotropic Ginzburg-Landau-Abrikosov-Gor'kov theory, resulting in $\xi_0=4\times 10^{-8}$ m and $\lambda(0)=1.2\times 10^{-7}$.

The fact that $\mu_0 H_{c2}$ of $ThPt_4Ge_{12}$ is substantially smaller than that of isomorphous $\{Sr,Ba\}Pt_4Ge_{12}$ $[\mu_0 H_{c2}(Sr)\approx -0.275$ T/K, $\mu_0 H_{c2}(Ba)\approx -0.46$ T/K$]$[1] might be a consequence of the observed variation of the Sommerfeld value γ and the residual resistivity ρ_0. Hake[19] and Orlando *et al.*[20] derived a model equation for $\mu_0 H_{c2}$ which primarily depends on two parameters: on the inverse of the square of v_F and on the inverse of l_{tr}. Both of these parameters are larger in the case of $ThPt_4Ge_{12}$, explaining straightforwardly the reduced value of $\mu_0 H_{c2}$. The Fermi velocity v_F of $ThPt_4Ge_{12}$ can be calculated from $v_F=\xi_0 k_B T_c/(0.18\hbar)=1.36\times 10^5$ m/s. Combining the Fermi-surface area S_s and ρ_0 as shown by Orlando *et al.*,[20] a mean-free path $l_{tr}\approx 6.5\times 10^{-8}$ m is derived. While the increase in v_F from the Ba ($v_F=0.52\times 10^5$ m/s) to the Sr ($v_F=0.67\times 10^5$ m/s) [1] and finally to the Th compound can be conceived by the increase in the unit-cell volume $[v_F\propto(N/V)^{1/3}$ for free electrons], the increase in the mean-free path corresponds to the very low residual resistivity ($\rho_0=3$ $\mu\Omega$ cm) of $ThPt_4Ge_{12}$. The importance of the latter parameter is obvious from $\mu_0 H_{c2}=$const $\gamma\rho_0$,[20] which is valid within the dirty limit case (const is a numerical constant).

From $l_{tr}/\xi\approx 1$ we classify $ThPt_4Ge_{12}$ as a SC grouped between the clean ($l_{tr}\gg\xi$) and the dirty ($l_{tr}\ll\xi$) limit; κ of the order of 3 refers to a type II superconducting behavior.

The temperature-dependent specific heat C_p of UPt_4Ge_{12} is plotted in Fig. 6(a) as C_p/T vs T. The absence of any low-temperature anomalies evidences the lack of a phase transition, in agreement with the $\rho(T)$ data indicated above. The inset in Fig. 6(a) shows C_p/T for T below 10 K. A standard procedure to isolate the magnetic contribution via

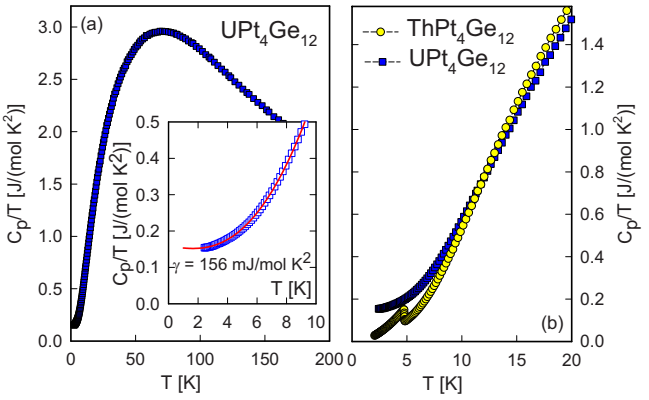

FIG. 6. (Color online) (a) Temperature-dependent specific heat C_p of UPt_4Ge_{12} plotted as C_p/T vs T. The inset shows low-temperature details and the solid line is a least-squares fit based on a spin fluctuation model. (b) Low-temperature heat capacity of $ThPt_4Ge_{12}$ and UPt_4Ge_{12} plotted as C_p/T vs T.

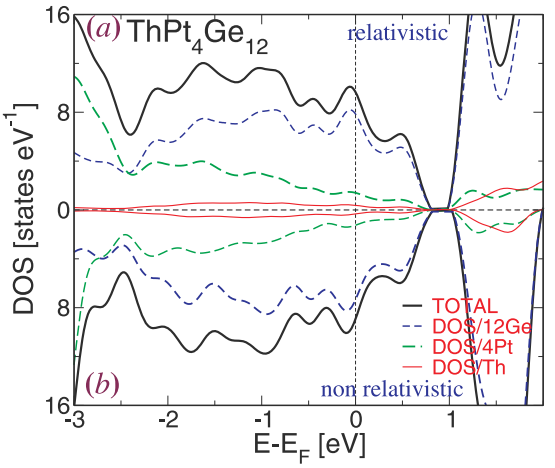

FIG. 7. (Color online) DOS for $ThPt_4Ge_{12}$ as derived from DFT calculations. Fermi energy is situated at zero energy. The upper half (a) shows the density of states for a fully relativistic calculation, which includes spin-orbit coupling. The lower half (b) of the figure presents the DOS of a standard nonrelativistic calculation. The total DOS is decomposed into the local DOS representative for one Th, four Pt, and twelve Ge atoms. The graphs clearly demonstrate the very dominant character of Ge states particularly at Fermi energy. These states are of expressed p-like character. The relativistic effect is small.

subtraction of $C_p(T)$ of isomorphous nonmagnetic $ThPt_4Ge_{12}$ fails since the C_p functions intersect each other, i.e., $C_p(T)$ of nonmagnetic $ThPt_4Ge_{12}$ surmounts that of UPt_4Ge_{12} for $T>12$ K [see Fig. 6(b)], referring to differences in the phonon spectrum. The observation of such a crossover is not a unique feature of the $\{U,Th\}Pt_4Ge_{12}$ systems but frequently occurs in isostructural pairs of {La, Ce} or complementary {Yb, LU} compounds. In all these cases, common explanations such as mass or volume differences do not apply, indicating rather a magnetic origin.

Although the phonon spectra of both compounds are more complex than that of a simple Debye solid, we attempted to fit the low-temperature data of UPt_4Ge_{12} with the ansatz $C_p(T)=\gamma T+\beta T^3+\delta T^3 \ln(T/T^*)$, where the latter term accounts for spin fluctuations. Satisfactory agreement is found for $\gamma=156$ mJ/mol K^2 and $T^*=2.7$ K [solid line, inset Fig. 6(a)], suggesting spin fluctuations in the nearly localized regime. The sizable value of γ in combination with the $\delta T^3 \ln(T/T^*)$ term, however, prevents to reliably derive β and thus the Debye temperature θ_D.

Albeit the combination of lattice and magnetic contributions does not allow a detailed analysis of lattice dynamics in UPt_4Ge_{12}. It should be noted that from temperature-dependent ADP parameters an Einstein mode for the U atoms was found at $\theta_E=59$ K, in close analogy to the phonon spectrum derived from the specific-heat analysis of $ThPt_4Ge_{12}$.

The calculated DOS, shown in Figs. 7(a) and 7(b), reveals the individual contributions of the Th, Pt, and Ge atoms, of which germanium p- and s-like states dominate the features of the DOS at E_F. The relativistic effect of spin-orbit coupling does not significantly influence the DOS at E_F. The directed covalent bonds of Ge intermixed with the more metal-like charge distribution of Pt states contribute to the peak of the DOS at E_F. From Bader's charge analysis,[21] about 0.13 electrons are transferred from each Ge to Pt, indicating only weakly ionic Pt-Ge bonds.

The total DOS at E_F can be compared with the Sommerfeld value of the specific heat $\gamma=\frac{1}{3}\pi^2 N(E_F)k_B^2$. The experimental values of about 35 mJ/mol K^2 for $ThPt_4Ge_{12}$ along with an electron-phonon enhancement factor $\lambda_{ep}=0.66$ (estimated via the McMillan formula[15]) would require a bare DOS equivalent of ≈ 21 mJ/mol K^2, which compares favorably with the DOS calculation involving spin-orbit coupling; 22.7 mJ/mol K^2 and $N(E_F)=9.63$ states eV^{-1} f.u^{-1}. Without spin-orbit coupling, $\gamma=20.1$ mJ/mol K^2, documenting the insignificance of relativistic effects.

For UPt_4Ge_{12}, however, the DFT calculations (not shown here) do not disclose any magnetic ordering, thereby confirming experimental observations. The total DOS at E_F of 16.21 states eV^{-1} f.u^{-1} is significantly larger than that of $ThPt_4Ge_{12}$. The corresponding Sommerfeld value $\gamma=38.2$ mJ/mol K^2 turns out to be smaller than the experimental value of 156 mJ/mol K^2 pointing toward the pronounced effect of spin fluctuations.

IV. SUMMARY

The $\{Th,U\}Pt_4Ge_{12}$ compounds are further representatives of family of skutterudites with a $[Pt_4Ge_{12}]$ sublattice. Resistivity, magnetic-susceptibility and specific-heat measurements indicate a phonon-mediated superconducting state in $ThPt_4Ge_{12}$ below $T_c=4.75$ K.

Superconducting properties of $ThPt_4Ge_{12}$ have been analyzed in detail [$\mu_0 H_{c2}(0)=0.21$ T, $\xi_0=4\times10^{-8}$ m, $\lambda(0)=1.2\times10^{-7}$], characterizing $ThPt_4Ge_{12}$ as a type II superconductor in the proximity of the clean limit. UPt_4Ge_{12} is dominated by spin fluctuations at low temperatures, preventing magnetic order and SC. DFT calculations proved the hybridization between Ge 4p-like and Pt 5d-like states in an energy

region around the Fermi level, dominating the DOS at E_F. Consequently, SC arises primarily from the electronic $[Pt_4Ge_{12}]$ sublattice states while Th (and U) plays a key role to electronically stabilize these skutterudites.

During revision of the paper we learned that SC in $ThPt_4Ge_{12}$ was recently also discovered by Kaczorowski and Tran.[22]

ACKNOWLEDGMENTS

Work supported by the Austrian science foundation FWF Projects No. P18054 and No. P16778/2. X.Q.C. is grateful to the partial support of the National Nature Science Fund of China (Project No. 50604004). P.R. is grateful to COST P16 "ECOM" for a short term mission in ITN.

[1] E. Bauer, A. Grytsiv, Xing-Qiu Chen, N. Melnychenko-Koblyuk, G. Hilscher, H. Kaldarar, H. Michor, E. Royanian, G. Giester, M. Rotter, R. Podloucky, and P. Rogl, Phys. Rev. Lett. **99**, 217001 (2007).

[2] A. Grytsiv, Xing-Qiu Chen, N. Melnychenko-Koblyuk, P. Rogl, E. Bauer, G. Hilscher, H. Kaldarar, H. Michor, E. Royanian, R. Podloucky, M. Rotter, and G. Giester, J. Phys. Soc. Jpn. **77**, 121 (2008).

[3] E. Bauer, A. Grytsiv, X.-Q. Chen, N. Melnychenko-Koblyuk, G. Hilscher, H. Kaldarar, H. Michor, E. Royanian, M. Rotter, R. Podloucky, and P. Rogl, Adv. Mater. (Weinheim, Ger.) **20**, 1325 (2008).

[4] R. Gumeniuk, W. Schnelle, H. Rosner, M. Nicklas, A. Leithe-Jasper, and Yu. Grin, Phys. Rev. Lett. **100**, 017002 (2008).

[5] V. Sechovsky and L. Havela, in *Handbook of Magnetic Materials, Volume 11*, edited by K. H. J. Buschow, Elsevier, Amsterdam, 1998, p. 1.

[6] G. Kresse and J. Furthmüller, Comput. Mater. Sci. **6**, 15 (1996).

[7] G. Kresse and J. Furthmüller, Phys. Rev. B **54**, 11169 (1996).

[8] P. E. Blöchl, Phys. Rev. B **50**, 17953 (1994).

[9] G. Kresse and D. Joubert, Phys. Rev. B **59**, 1758 (1999).

[10] J. P. Perdew, K. Burke, and M. Ernzerhof, Phys. Rev. Lett. **77**, 3865 (1996).

[11] W. Jeitschko and D. J. Braun, Acta Crystallogr., Sect. B: Struct. Crystallogr. Cryst. Chem. **33**, 3401 (1977).

[12] D. W. Woodard and G. D. Cody, Phys. Rev. **136**, A166 (1964).

[13] A. Junod, D. Bichsel, and J. Mueller, Helv. Phys. Acta **52**, 580 (1979).

[14] A. Junod, T. Jarlborg, and J. Muller, Phys. Rev. B **27**, 1568 (1983).

[15] W. L. McMillan, Phys. Rev. **167**, 331 (1968).

[16] N. R. Werthamer, E. Helfand, and P. C. Hohenberg Bell, Phys. Rev. **147**, 295 (1966).

[17] K. Maki, Phys. Rev. **148**, 362 (1966).

[18] K. M. Wong, E. J. Cotts, and S. J. Poon, Phys. Rev. B **30**, 1253 (1984).

[19] R. R. Hake, Phys. Rev. **158**, 356 (1967).

[20] T. P. Orlando, E. J. McNiff, Jr., S. Foner, and M. R. Beasley, Phys. Rev. B **19**, 4545 (1979).

[21] G. Henkelman, A. Arnaldsson, and H. Jónsson, Comput. Mater. Sci. **36**, 254 (2006).

[22] D. Kaczorowski and V. H. Tran, Phys. Rev. B **77**, 180504(R) (2008).